IR−UV Double-Resonance of Methyl Radicals and a Determination of the Detection Sensitivity of REMPI Bands†

Weiqing Zhang,‡,§ Hiroshi Kawamata,§ Anthony J. Merer,|| and Kopin Liu*

Institute of Atomic and Molecular Sciences (IAMS), Academia Sinica, P.O. Box 23-166, Taipei, Taiwan 10617

Received: April 1, 2009; Revised Manuscript Received: May 9, 2009

A novel method is exploited in this report to directly determine the relative detection sensitivity of the (2+1) resonance-enhanced multiphoton ionization (REMPI) bands of CH_3 and CHD_2 radicals. The basic idea is based on the simple fact that in an infrared (IR) absorption process the number of molecules being pumped from the lower state must be the same as the number of molecules in the excited upper state. Hence, the measured intensities of the respective REMPI bands should directly reflect their relative detection sensitivities. In order to ensure the processes involved and better quantify the measurements, extensive IR−UV double resonance spectroscopy was also performed. Using the REMPI-IR scheme, the IR spectrum of the υ_1 fundamental (CH stretch) of CHD_2 was obtained and assigned for the first time. Using the IR-REMPI approach, high-resolution (2+1) REMPI spectra via the Rydberg 3p states of both radicals were demonstrated in a rotationally specific manner for both the origin and vibronic-excited bands, from which the predissociation rates of the Rydberg 3p states were deduced.

I. Introduction

The methyl radical stands at a unique position as a prototype for the entire family of alkyl radicals and serves as a benchmark for theoretical calculations aimed at fundamental understanding of the physical and chemical properties of this class of open-shell systems. It is also an important intermediate in many chemical processes of environmental and industrial interest, such as hydrocarbon combustion,[1] atmospheric chemistry,[2] and chemical vapor deposition of diamond films.[3] Because of its fundamental properties and practical importance, the methyl radical has been the subject of numerous experimental[4−20] and theoretical investigations.[21−23] Considerable efforts have been made to develop sensitive and selective detection schemes for diagnostic applications.[4−19] Among them, (2+1) resonance-enhanced multiphoton ionization (REMPI) spectroscopy is clearly a viable method. In particular, the REMPI process using the 3p Rydberg intermediate state has become very popular in recent studies of chemical dynamics,[7−14] thanks to the sensitive probes of not only the vibrational ground state but several vibrationally excited states.[11−14] To gain deeper insights into the dynamical processes of interest and to allow more direct comparison with theory, however, one also needs to quantify the relative detection sensitivities of the observed REMPI vibronic bands. Due to the experimental difficulties and limitations, the only previous attempt for such a determination was for the umbrella-excited $CD_3(\upsilon_2 = 1, 2,$ and $3)$ states with respect to the ground state $CD_3(\upsilon = 0)$.[12] The method employed in that report was somewhat tedious and depended on a kinetic modeling of the REMPI process, calling for an alternative approach that is also applicable to the other vibronic bands.

Double-resonance spectroscopy has a long history and is a powerful experimental technique to decipher complicated and congested spectra. With the advent of new laser sources, a wide range of combinations spanning from microwave to vacuum ultraviolet (VUV) has been exploited—too numerous to be cited here. In addition to the high-resolution spectroscopic works, this technique has been extended to investigating the isomerization processes,[24,25] intramolecular vibrational energy redistribution (IVR) dynamics,[26,27] cluster dynamics,[28,29] and collision-induced energy transfer processes[30,31]—just to name a few. Added to the long list is this work on the use of double-resonance spectroscopy to directly determine the relative detection sensitivity of the vibronic bands in a REMPI process. Specifically, we demonstrated its feasibility for both the 3^1_1 band of the $CH_3(3p_z\ ^2A \leftarrow X\ ^2A'')$ REMPI transition and the 1^1_1 band of the $CHD_2(3p\ ^2B_1 \leftarrow X\ ^2B_1)$ transition.

II. Experiment

The experiments were performed using the crossed-beam apparatus described in detail previously,[12−14,32] except that only a single beam was used in this work. The methyl radicals were generated by discharging a gas mixture of methane released from a fast-opening piezoelectric transducer (PZT) pulsed valve.[33] Typical discharge high-voltage was 1 kV and two gas mixtures at stagnation pressures of 6 atm were used in this work: (5% CH_4 + 5% CD_4) seeded in He mainly for identifying the IR spectra, and (1% CH_4 + 1% CD_4 + 20% Ar) seeded in He, which yielded a colder rotational distribution, for quantifying the relative detection sensitivity. Both mixtures yield methyl radicals in all isotopic forms.

Figure 1 shows the pump−probe schemes for REMPI-IR and IR-REMPI spectroscopy. The notation of REMPI-IR means that the UV wavelength in REMPI is fixed while the IR frequency is scanned, and vice versa for IR-REMPI. The selected rovibrational state of the $CH_3(X\ ^2A_2'')$ or $CHD_2(X\ ^2B_1)$ radicals was pumped by a tunable IR optical parametric oscillator/amplifier (OPO/A, LaserVision) near 3 μm at 20 Hz. Its absolute wavelength was calibrated against a $CH_4(\upsilon_3 = 1 \leftarrow 0)$ photoa-

† Part of the "Robert W. Field Festschrift".

* Corresponding author. E-mail: kliu@po.iams.sinica.edu.tw.

‡ State Key Laboratory of Molecular Reaction Dynamics, Dalian Institute of Chemical Physics, CAS, P.O. Box 110 ext. 11, Dalian 116023, P. R. China.

§ These authors contributed equally to this work.

|| Also Department of Chemistry, University of British Columbia, Vancouver, B.C., Canada V6T 1Z1.

10.1021/jp902969v CCC: $40.75
Published on Web 06/04/2009

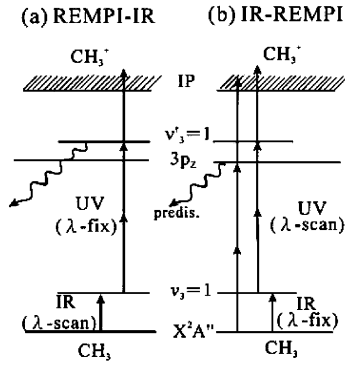

Figure 1. Schematic diagrams of (a) REMPI-IR and (b) IR-REMPI double-resonance spectroscopy methods. REMPI-IR is used to identify the IR spectrum of the electronic ground state of the methyl radical, whereas IR-REMPI is exploited to measure the REMPI detection sensitivity.

coustic spectrum. The IR excitation laser was coupled to a multipass ring-reflector situated just in front of the first skimmer in the source chamber.[34] Judging from the IR-power dependence of the observed ion signals, the IR transition was clearly saturated. Despite the resultant power broadening ($\sim$0.2 cm^{-1} in width), the REMPI-IR spectra display well-resolved individual (N, K)-transitions. The probe radiation near 334 nm in the REMPI process was the frequency-doubled output of a dye laser and was directed into a differentially pumped scattering chamber. A wavemeter reads the absolute frequency of the dye laser output. The time delay between the IR and UV lasers was typically 107 μs for both gas mixtures. The REMPI-generated ions were then detected by the ion imaging technique in the spatial mode of operation. Note that the 100 μs delay time is long enough for hyperfine depolarization to scramble the initial alignment of IR excitation. Yet, it is significantly shorter than the radiative lifetime of the vibrationally excited state, which was estimated to be tens of seconds as a result of the small υ_3-transition dipole moment (0.029 D)[35] of the CH_3 radical; thus the IR-excited radicals are essentially intact when the UV probe laser is fired.

In the REMPI-IR scheme shown in Figure 1a, the UV probe laser frequency is fixed at a targeted vibronic band while the IR laser frequency is scanned. We take advantage of the spectral congestion of the Q-head of the REMPI band to yield essentially the IR absorption spectrum of the methyl radical. To determine the relative REMPI detection sensitivity, we turned to the IR-REMPI approach. In this scheme, the IR excitation is fixed at a particular $\upsilon = 1 \leftarrow 0$, $N'_{K'} \leftarrow N''_{K''}$ transition and the UV laser frequency scanned. [For clarity, we will use double- and single-prime superscripts in labeling the rotational quantum states of the lower and the upper states of the IR transition, respectively; no superscript for the 3p Rydberg state.] Both the depletion (i.e., attenuation) of the REMPI 0_0^0-band and the formation (or enhancement) of the ν_1^1-band could then be observed. Since the amount of molecules being depleted, $\Delta n(0_0^0)$, should be the same as the amount of molecules being excited, $\Delta n(\nu_1^1)$, the observed difference in the respective differential REMPI intensities ΔI should then reflect the relative detection sensitivity S, i.e.,

$$\Delta n(0_0^0) = |\Delta I(0_0^0)|/S(0_0^0) = \Delta n(\nu_1^1) = \Delta I(\nu_1^1)/S(\nu_1^1) \quad (1)$$

or

$$S(\nu_1^1)/S(0_0^0) = \Delta I(\nu_1^1)/|\Delta I(0_0^0)| \quad (2)$$

Here, ΔI is defined as the REMPI signal I for IR-on minus that for IR-off; thus, an absolute value of $|\Delta I(0_0^0)|$ is taken to account for the attenuation.

To better quantify $S(\nu_1^1)/S(0_0^0)$, the peak height measurements were also recorded, in which the UV frequencies were repeatedly fixed at the peak of the 0_0^0 and ν_1^1 bands and the signals recorded with the IR alternating on and off. While the sensitivity determination in this work refers to a linearly polarized UV laser beam, a circularly polarized UV probe laser was also used to facilitate the spectral identification.

III. Results and Discussion

A. IR−UV Double Resonance Spectroscopy of the CH_3 Radical. The ground electronic state of $CH_3(X\,^2A'')$ has a planar geometry with D_{3h} symmetry.[4] Being a symmetric top, its rotational energy levels are characterized by the quantum numbers N (end-over-end tumbling) and K (projection on body axis), denoted as N_K. The presence of three identical protons (Fermi statistics, spin = $^1/_2$) results in three different nuclear spin modifications A_1, A_2, and E with the statistical weights of 10, 1, and 8, respectively.[36] Figure 2a shows a portion of the REMPI-IR spectrum of CH_3. The UV laser frequency was fixed at the half of 59 881 cm^{-1} (in vacuo) to excite the 3_1^1 band of the $3p_z\,^2A'' \leftarrow X\,^2A''$ transition,[11] which is about 76 cm^{-1} red-shifted from the origin band 0_0^0. The $\upsilon_3 = 1$ state accessed by the IR excitation is doubly degenerate. Coriolis coupling breaks this degeneracy, resulting in characteristic l-type doubling.[16] The high-resolution IR spectrum of the $CH_3(\upsilon_3 = 1 \leftarrow 0)$ transition, with $\upsilon_0 = 3160.82$ cm^{-1}, has been well studied.[16−18] The spectral features shown in Figure 2a can readily be assigned and the observed relative spacings are all within 0.05 cm^{-1} of literature values.

Figure 3a presents the IR-REMPI spectrum recorded using linearly polarized UV light with the IR radiation fixed at the CH_3, $\upsilon_3 = 1 \leftarrow 0$, 2_1-2_0 transition (3154.8 cm^{-1}). Two remarks are in order. First, comparing the relative intensities of the two spectra, black for IR-off and red for IR-on, the formation of the 3_1^1 Q-branch and the small attenuation of the 0_0^0 Q-head can be seen. [The small depletion, in terms of percentage, of the 0_0^0 Q-head is due to the state-dilution effect: The IR laser excites a single $\upsilon = 0$, $N''_{K''} = 2_0$ state, whereas the 0_0^0 Q-head comprises the contributions from many rotational states (despite the low rotational temperature in the supersonic beam) and for which different nuclear spin modifications are not interconvertible by supersonic relaxation.] Both the 0_0^0 attenuation and 3_1^1 formation are anticipated; however, a small peak near 59 842 cm^{-1} is discernible in the IR-on spectrum.

To shed more light on this peak, Figure 3b shows the IR-REMPI spectrum using a circularly polarized UV light instead. It is known that in the (2+1) REMPI process of a symmetric top molecule, the Q-branch gains additional intensity factor from the zero rank component of the two-photon transition tensor when using a linearly polarized laser (thus, significantly increasing its detection sensitivity), whereas the intensities of the other branches (O, P, R, and S) are enhanced for circularly polarized light by a factor of 1.5.[37] Indeed, inspection of Figure 3a,b indicates a factor of 4−5 drop in the 0_0^0 Q-intensities, which is compared to a factor of about 14 found previously for $CD_3(0_0^0$ Q) and $CD_3(2_2^0$ Q).[38] [We note that the polarization dependence of the 3_1^1 Q-branch seems more dramatic because the only spectral feature left near 59 880 cm^{-1} in Figure 3b is the

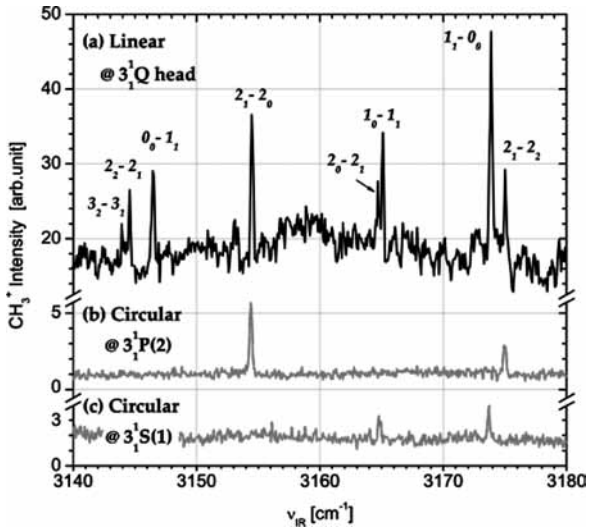

Figure 2. IR spectra of CH_3, acquired by the REMPI-IR scheme, in the region of the fundamental of antisymmetric stretch (υ_3) when (a) the wavelength of a linearly polarized UV light is fixed at the peak of the 3_1^1 Q-head of the REMPI transition, (b) the wavelength for a circularly polarized UV light is fixed at the 3_1^1 P(2) peak, and (c) the wavelength of a circularly polarized UV light is fixed at the 3_1^1 S(1) peak. The elevated baseline in (a) clearly reduces the S/N ratio.

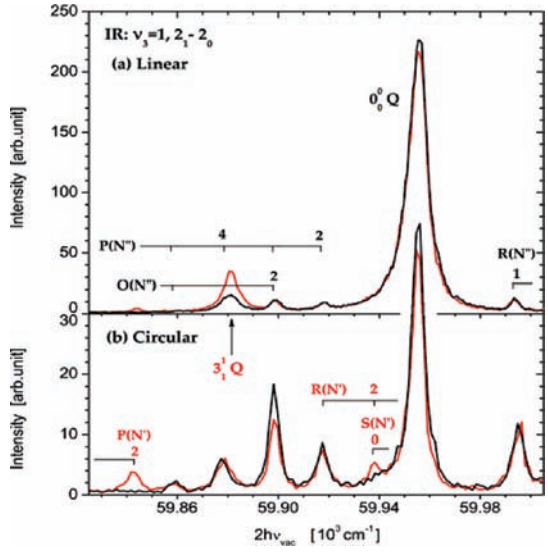

Figure 3. REMPI spectra of CH_3, acquired by the IR-REMPI method, with either (a) linearly polarized or (b) circularly polarized UV light. The IR pumping transition is $\upsilon_3 = 1 \leftarrow 0$, $2_1 \leftarrow 2_0$, and the red (black) line is for IR-on (IR-off). Color codes in the rotational branch assignment are black for the electronic origin band 0_0^0 and red for the vibrationally excited 3_1^1 band.

overlapped 0_0^0 P(4) transition.] In addition, the attenuation of the 0_0^0 O(2) intensity due to the 2_1-2_0 (IR) excitation becomes more obvious. As to the 59 842 cm^{-1} peak, we assign it to the 3_1^1 P(2) REMPI transition. To confirm this assignment, we fixed the UV laser at 59 842 cm^{-1} while scanning the IR frequency. The resultant REMPI-IR spectrum is presented in Figure 2b. Clearly, only two IR transitions were observed and both indicate excitation to the $\upsilon_3 = 1$, $N' = 2$ state, thus confirming the 59 842 cm^{-1} peak assignment. It is worth noting the observation of a small IR-on peak near 59 938 cm^{-1} in Figure 3b, which is apparently overwhelmed in Figure 3a by the tail of the intense 0_0^0 Q-head. Similarly, the REMPI-IR spectrum (not shown) was acquired for its identification, and three peaks were observed. In addition to the anticipated 2_1-2_0 and 2_1-2_2 peaks, which

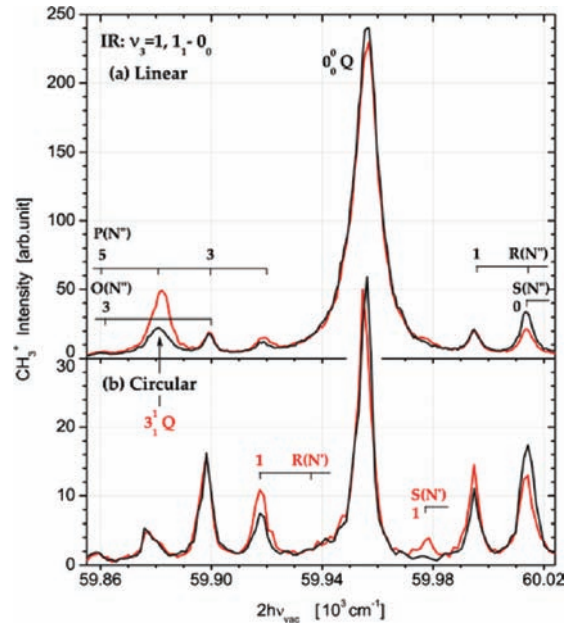

Figure 4. As in Figure 3, except that the $\upsilon_3 = 1 \leftarrow 0$, $1_1 \leftarrow 0_0$ IR transition is used.

turned out to be rather minor, the dominant peak in the IR spectrum corresponds to the 0_0-1_1 transition. Hence the small REMPI feature at 59 938 cm^{-1} is assigned to the overlapped R(2) and S(0) transitions of the 3_1^1 REMPI band, which is similar to the 0_0^0 case.

Second, taking the difference of the IR-on and IR-off spectra in Figure 3, one can obtain the IR-activated 3_1^1 Q, P(2), and S(0)/R(2) peaks and the attenuated 0_0^0 Q and O(2) features. All display an approximate width of 5 cm^{-1}, which is significantly larger than that of the dye laser (<0.1 cm^{-1}) or the fine structure splittings.[15−18] Since those peaks correspond to a single IR transition of ($\upsilon_3 = 1 \leftarrow 0$, 2_1-2_0), we attribute the spectral width as a manifestation of the lifetime broadening of the predissociating $3p_z\ ^2A''$ intermediate state,[7,8,12] from which the total decay rate, i.e., the predissociation plus the (third-photon) ionization, of $\sim 1.5 \times 10^{11}$ s^{-1} is estimated for both $\upsilon = 0$ and $\upsilon_3 = 1$ excitations of the $3p_z\ ^2A''$ Rydberg state. The UV laser power used was about 6 mJ in 3 ns and mildly focused by a $f = 50$ cm cylindrical lens. Assuming a photoionization cross section of 10^{-17} cm^2 from the $3p_z\ ^2A''$ Rydberg state, the rate of ionization is merely 3×10^9 s^{-1}. Obviously, the observed spectral width is dominated by the predissociation process. Moreover, the same width was observed from either the formation of 3_1^1 lines or the attenuation of the 0_0^0 transitions, indicating a similar predissociation rate for the two vibronic states. Intuitively, one might have anticipated a faster predissociation rate from a stretch-excited Rydberg state, leading to $CH_2 + H$ fragments, by analogy to the predissociation of the Rydberg 3s B-state of CH_3. Previously a far-UV resonance Raman spectroscopic study of the 3s B-state reported a predissociation rate of $\sim 1.2 \times 10^{13}$ s^{-1} for $\upsilon = 0$, with a slight dependence on the rotational state.[39] The rate increases to about 6×10^{13} s^{-1} upon one quantum excitation of the symmetric stretching mode ($\upsilon_1 = 1$).[40]

Similar IR-REMPI experiments were performed via the 1_1-0_0 IR line at $\upsilon_{IR} = 3174.3$ cm^{-1}. As presented in Figure 4, two new peaks were observed with IR-on and were assigned to the REMPI transitions 3_1^1 R(1) at 59 918 cm^{-1} and 3_1^1 S(1) at 59 977 cm^{-1}. Again, their assignments were facilitated by the REMPI-IR spectrum, as illustrated in Figure 2c for the 3_1^1 S(1) case.

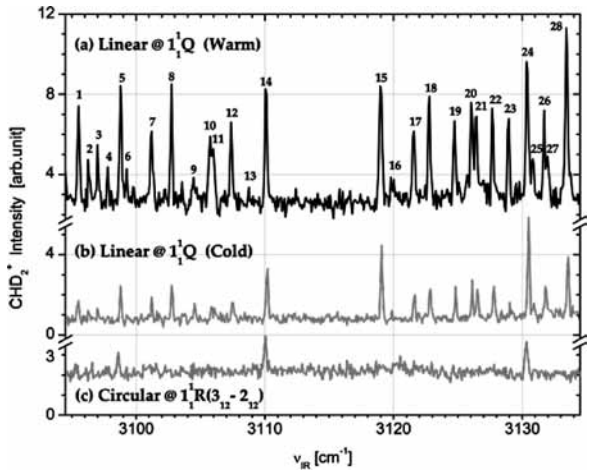

Figure 5. υ_1 fundamental of the CHD_2 radical, recorded as in Figure 2. The peak assignments are listed in Table 1.

Due to both the intrinsic REMPI spectral width (~5 cm^{-1}) and the small number of observed transitions [only P(2), S(0)/R(2), R(1), and S(1)], no further rotational analysis was performed. Nevertheless, within the limited resolution, the rotational constants of the $3p_z$ $^2A''$ Rydberg state appear quite similar to the ground state X $^2A''$. In passing, Figures 3 and 4 also provides a clear illustration of a way to decipher the *K*-overlapped substructure of a REMPI feature.

B. IR Spectrum of the $\upsilon_1 = 1 \leftarrow 0$ Transition of the $CHD_2(X\ ^2B_1)$ Radical. In contrast to the CH_3 radical, no high-resolution spectroscopy has been reported for the CH stretching fundamental of CHD_2, though a far-UV resonance Raman spectrum[41] has given an approximate value, $\upsilon_1 = 3116.2$ cm^{-1}. By fixing the two-photon UV laser frequency at the 1^1_1 band position (~58 943 cm^{-1}, or 78 cm^{-1} to the red of the 0^0_0 band), and scanning the IR frequency, we have obtained the REMPI-IR spectra shown in Figure 5. The top spectrum, Figure 5a, was obtained by discharging the 5% CH_4/5% CD_4 gas mixture, which yields a warmer beam, giving more rotational lines. The colder spectrum of Figure 5b was obtained by discharging the 1% CH_4/1% CD_4/20% Ar/He mixture which had been used in the relative detection sensitivity measurements. Compared to the REMPI-IR spectra of CH_3 shown in Figure 2, the spectra of CHD_2 are clearly more complicated.

CHD_2 is a planar asymmetric top with C_{2v} symmetry. Its 2-fold symmetry axis is the inertial B axis, and the inertial A axis is parallel to a line joining the two D atoms. The CH stretching fundamental υ_1 (a_1 vibrational symmetry) is therefore a B-type band. Its rotational structure shows an intensity alternation resulting from the nuclear spins of the two equivalent deuterium atoms. Because the electronic ground state has $^2B_1$ symmetry, the alternation is such that lines arising from levels with $K_a + K_c =$ odd (B_1 and B_2 rotational symmetry) have twice the intensity of those from levels with $K_a + K_c =$ even (A_1 and A_2 rotational symmetry).[36] As expected by analogy with CH_3, the electron spin splittings are not large enough to be observable at our resolution.

The spectrum shown in Figure 5a could be assigned from calculations of the rotational structure. A preliminary set of rotational constants was calculated, assuming that the bond angles are 120°, and that all the bond lengths are 1.076 Å, as in the vibrational ground state of CH_3.[17] These constants were $A = 7.15$ cm^{-1}, $B = 4.63$ cm^{-1}, and $C = 2.81$ cm^{-1}. The rotational structure of the band could then be predicted approximately, assuming that the rotational constants do not change on vibrational excitation. The prediction reproduced the relative positions of the lines to within about 0.5 cm^{-1}, which is sufficiently close that the rotational assignments could be made without difficulty, taking account of the intensity alternation. An energy level diagram, illustrating the B type selection rules for some of the lowest rotational levels, is given as Figure 6.

TABLE 1: Observed Transitions of the υ_1 Band of $CHD_2(X\ ^2B_1)$ Radical and the Spectral Assignments[a]

	upper state ($\upsilon_1 = 1$)	lower state ($\upsilon = 0$)
T_0	3114.577 ± 0.073	0 (fixed)
A	7.137 ± 0.021	7.192 ± 0.021
B	4.651 ± 0.018	4.678 ± 0.019
C	2.803 ± 0.015	2.809 ± 0.014
	rms error = 0.056 cm^{-1}	

peak no.	assignment	obs	obs − calc
1	$P(2_{12}-3_{03})$	3114.46−18.70	0.0
2	$Q(3_{22}-3_{31})$	−17.90	−0.04
3	$P(2_{21}-3_{12})$	−17.24	0.04
4	$Q(3_{13}-3_{22})$	−16.43	−0.04
5	$P(1_{01}-2_{12})$	−15.49	0.04
6	$Q(3_{21}-3_{30})$	−14.92	0.07
7	$Q(2_{12}-2_{21})$	−13.09	0.05
8	$P(1_{11}-2_{02})/Q(3_{03}-3_{12})$	−11.6	0.08
9	$P(0_{00}-1_{11})$	−9.90	−0.02
10	$Q(3_{12}-3_{21})$	−8.60	0.0
11	$Q(2_{11}-2_{20})$	−8.40	−0.09
12	$Q(2_{02}-2_{11})$	−7.00	−0.05
13	$P(2_{20}-3_{13})$	−5.60	−0.06
14	$Q(1_{01}-1_{10})$	−4.38	−0.08
15	$Q(1_{10}-1_{01})$	+4.38	−0.04
16	$R(3_{13}-2_{20})$	+5.40	0.05
17	$Q(2_{11}-2_{02})$	+7.00	0.07
18	$Q(2_{20}-2_{11})/Q(3_{21}-3_{12})$	+8.18	0.06
19	$R(1_{11}-0_{00})$	+10.09	0.03
20	$Q(3_{12}-3_{03})$	+11.40	0.0
21	$R(2_{02}-1_{11})$	+11.70	−0.06
22	$Q(2_{21}-2_{12})$	+13.00	−0.01
23	$Q(3_{30}-3_{21})$	+14.22	−0.07
24	$R(2_{12}-1_{01})$	+15.66	0.03
25	$Q(3_{22}-3_{13})$	+16.10	−0.01
26	$R(3_{12}-2_{21})$	+16.98	0.01
27	$Q(3_{31}-3_{22})$	+17.24	0.04
28	$R(3_{03}-2_{12})$	+18.67	0.0

[a] The notation in parentheses indicates the rotational quantum numbers $N'_{K'aK'c} - N''_{K''aK''c}$. All frequencies are in cm^{-1}, and the peak no. refers to Figure 5. Rotational constants from least squares fitting of the observed lines of the υ_1 band of CHD_2 (values in cm^{-1}) are listed first. The quoted error limits are three standard deviations.

A full least-squares fit was then carried out. Since the values of *N* and *K* go only up to 3, the energy levels were calculated using just the rigid rotator matrix elements, without centrifugal distortion terms:[42]

$$\langle NK|H_{rot}|NK\rangle = [A - 1/2(B + C)]K^2 + 1/2(B + C)N(N + 1) \quad (3)$$

$$\langle NK|H_{rot}|NK \pm 2\rangle = 1/4(B - C)[N(N + 1) - K(K \pm 1)]^{1/2}[N(N + 1) - (K \pm 1)(K \pm 2)]^{1/2} \quad (4)$$

The final rotational constants are given in Table 1, along with the assigned line frequencies and the residuals from the fitting. The rms error was 0.056 cm^{-1}, which is comparable to the

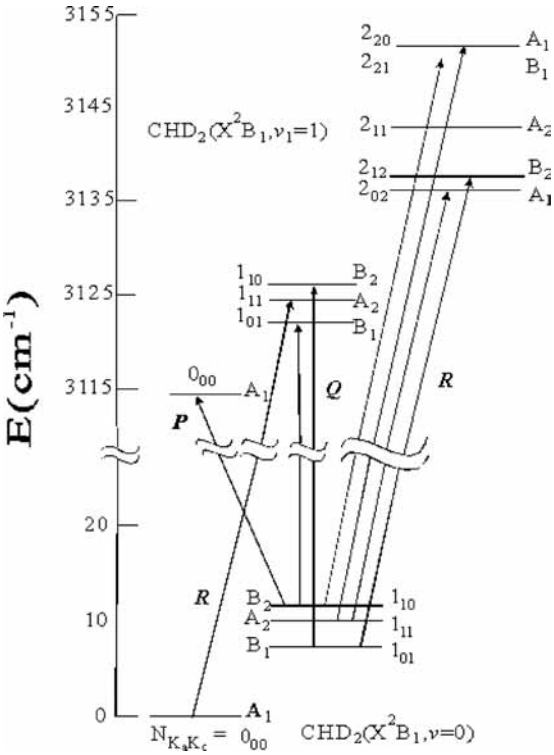

Figure 6. Schematic energy level diagram of the rotational energy levels for both the ground and $v_1 = 1$ excited states of CHD_2. Besides the quantum number labeling, the rotational symmetry species of each state is also indicated. The B-type dipole allowed transitions from the lowest two *N*-levels are marked.

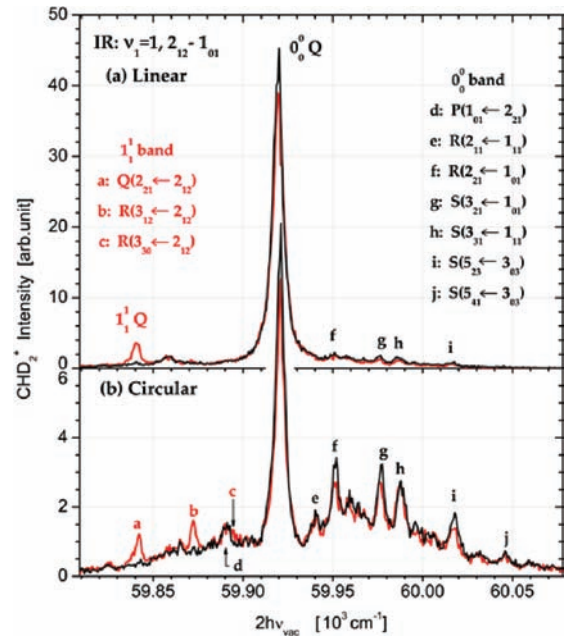

Figure 7. As in Figure 3, but for CHD_2. The IR pumping transition is $v_1 = 1 \leftarrow 0, 2_{12} \leftarrow 1_{01}$. Tentative assignments of the rotationally resolved REMPI transitions are indicated.

accuracy of the measurements. The upper state constants are very similar to those of the ground state, with the only significant difference being a slight decrease in the *A* rotational constant on vibrational excitation. This is consistent with the expected slight lengthening of the CH bond on excitation. Because the changes in the rotational constants are comparatively small, the band shows a remarkable mirror symmetry around the band origin, which is clearly seen in Figure 5.

It will be interesting to have confirmation of these rotational constants from spectra taken at higher resolution in the future. To date, the only reported rotational constants for CHD_2, $\tilde{X}\ ^2B_1$, $v = 0$ are from photoionization work using threshold photoelectron spectroscopy.[43] Unfortunately, these constants ($A = 7.60$ cm^{-1}, $B = 4.91$ cm^{-1}, and $C = 2.89$ cm^{-1}) are not consistent with the results of the present work, since they lead to combination differences which disagree with those observed in the infrared by over 5%.

The IR-REMPI spectra for the CHD_2 radical are presented in Figure 7, for which the IR frequency was fixed at 3130.7 cm^{-1} in order to excite the $v_1 = 1 \leftarrow 0, 2_{12}-1_{01}$ transition (peak 24). It is clear from the spectra shown in Figure 7a,b that even for the present asymmetric rotor the intensity of the Q-head drops by about 5-fold on changing the UV probe-laser polarizations. The formation of new peaks with $v_1 = 1, 2_{12}$ as the lower state (a, b, and c) and the attenuation from the depleted $v = 0$, 1_{01} level (0_0^0 Q-branch, f and g) are both observed. [The attenuation of peak-i in Figure 7b is uncertain because it is not reproducible and it gives a negative result in the REMPI-IR search.] From the difference spectrum between the IR-on and IR-off (not shown), a width of about 5 cm^{-1} was obtained for both the enhanced peaks and the ion-dip features, which is essentially an identical value to the CH_3 case. REMPI-IR spectroscopy was then exploited to facilitate the spectroscopic assignment of the new peaks in the IR-on spectra. Illustrated in Figure 5c is the case for which the UV frequency was fixed at 59 877 cm^{-1}, exciting peak-b. In addition to the anticipated $R(2_{12}-1_{01})$ transition (peak 24), two more IR transitions were recorded (peak 5 and 14), corresponding to $P(1_{01}-2_{12})$ and $Q(1_{01}-1_{10})$, respectively. It then suggests that another REMPI transition originating from the IR-excited ($v_1 = 1$, 1_{01}) state must occur near 59 877 cm^{-1}. Using the known rotational level pattern for the ground state, and assuming a similar one for the 3p $^2B_1$ Rydberg state, the anticipated REMPI frequencies of the various transitions can be calculated. In this calculation the two-photon selection rules, $A_1 \leftarrow A_1$, $A_2 \leftarrow A_2$, $B_1 \leftarrow B_1$, and $B_2 \leftarrow B_2$, were used. On that basis, we assigned the overlapped REMPI transition as 1_1^1 $R(2_{21}-1_{01})$. Within an accuracy of 2 cm^{-1} (in the UV), a tentative assignment of all observed major REMPI peaks can now be made, as listed in Figure 7.

C. REMPI Detection Sensitivities of the $CH_3(3p_z\ ^2A'' \leftarrow X\ ^2A'', 3_1^1)$ and $CHD_2(3p\ ^2B_1 \leftarrow X\ ^2B_1, 1_1^1)$ Bands. Given our understanding of the IR−UV double-resonance spectra, we are in a position to measure the detection sensitivity of the REMPI bands by (1) repeating the IR-REMPI spectral scans and (2) recording the peak-height intensities of the 0_0^0 Q and 3_1^1 (or 1_1^1) Q-heads with the IR radiation alternating on and off. [The spectral scan in the first approach took typically half to one hour for one pair of IR-on and IR-off. To minimize the long-term drifts and to improve the statistics of measurements, in method 2 the depletion and the formation were alternatively monitored, and for each about five cycles of on/off pairs were measured and averaged.] Table 2 summarizes the results. Despite the large uncertainties (mainly because only a small fraction of the 0_0^0 Q-intensity can be depleted), the results for CH_3 obtained by using either the 1_1-0_0 or the 2_1-2_0 IR excitations are nearly the same, indicating little dependence on the rotational states of the two vibronic bands as well as negligible polarization effects since no difference was discernible from the R- and Q-branch pumping. On the other hand, all four sets of measurements yield a greater REMPI detection sensitivity of 3_1^1 Q than 0_0^0 Q, with the average of $S(3_1^1)/S(0_0^0) \approx 3.4 \pm 0.6$, which is somewhat surprising and puzzling. One plausible explanation

TABLE 2: REMPI Detection Sensitivities of the Vibronically Excited Bands, $CH_3(3_1^1)$ and $CHD_2(1_1^1)$, Relative to the Respective Origin Band 0_0^0 [a]

IR excitation	method	$S(\nu_i^1)/S(0_0^0) \pm$ std dev	no. of runs
$CH_3(\upsilon_3 = 1 \leftarrow 0)$	spectral area	2.4 ± 2.7	4
$2_1 - 2_0$	peak height	3.5 ± 0.7	20
		3.3 ± 0.7 [b]	
$CH_3(\upsilon_3 = 1 \leftarrow 0)$	spectral area	2.1 ± 2.3	4
$1_1 - 0_0$	peak height	4.1 ± 1.4	20
		3.5 ± 1.2 [b]	
$CHD_2(\upsilon_1 = 1 \leftarrow 0)$	spectral area	1.7 ± 1.0	6
$2_{12} - 1_{01}$	peak height	2.0 ± 1.2	20
	peak height	1.9 ± 1.1	20
		1.9 ± 0.7 [b]	

[a] The UV probe laser is linearly polarized. [b] Average value.

is as follows. Ab initio calculations indicated that the Franck−Condon factors for the 0_0^0 and 3_1^1 two-photon transitions are nearly the same.[23] Based on a simple kinetic model of the (2+1) REMPI process,[12] the differential sensitivity of the two bands must then arise from the fates of the respective Rydberg excited states. The probability of absorbing the third photon leading to ionization can be expressed as $k_I/(k_I + k_P)$, where k_I is the rate of ionization and k_p gives the rate of predissociation. As shown in section IIIA, $k_I + k_P \approx k_p$, which is, counterintuitively, about the same for both the $\upsilon_3 = 1$ and $\upsilon = 0$ levels of the $3p_z$ Rydberg state. Therefore, the higher sensitivity of $S(3_1^1)$, compared to $S(0_0^0)$, implies a faster ionization rate. Previously, a detailed analysis of the high resolution IR spectrum of CH_3^+ yielded a value of 1.095 Å for the C−H bond length,[44] which is significantly longer than those of CH_3 ($r_{C-H} = 1.076$ Å for the ground state[17] or 1.086 Å estimated from the rotational constants of the 3p Rydberg state[45]). It is conceivable that the faster k_I from the $\upsilon_3 = 1$ (C−H stretching excited) level of the Rydberg 3p state, compared to that from $\upsilon = 0$, originates from a more favorable Franck−Condon overlap in the ionization step.

Similar measurements were carried out for the REMPI 1_1^1 band of the CHD_2 radical. The results are also summarized in Table 2. The resultant detection sensitivity, $S(1_1^1)/S(0_0^0) \approx 1.9 \pm 0.7$, is again greater than 1, though slightly smaller than the CH_3 case. We proposed that a similar mechanism, a faster ionization rate for the stretch-excited Rydberg state, can account for the differential detection sensitivity.

IV. Conclusions

IR−UV double resonance spectroscopy is applied to study the REMPI detection of the methyl radicals CH_3 and CHD_2. Using the REMPI-IR scheme, we report the first rotationally resolved IR spectrum of $CHD_2(\upsilon_1 = 1 \leftarrow 0)$. With the IR-REMPI approach we demonstrate the possibility of obtaining a high-resolution REMPI spectrum with complete rotational specificity in both the upper and lower states, despite the intrinsic spectral congestion and broadening from the fast predissociation of the intermediate Rydberg state. In addition to the spectroscopic aspects, we have exploited the nature of the double-resonance technique to quantify the relative detection sensitivity of the REMPI vibronic bands. Such information is particularly valuable in putting the results obtained for the dynamical processes of interest in a proper perspective.[46] The basic idea of this approach is simple and quite general, provided that the state populations can be selectively transferred by a means such as IR absorption, Raman scattering, or even collision, etc.; thus it should be applicable to many other species.

Acknowledgment. This work was financially supported by the National Science Council of Taiwan, Academia Sinica, and the U.S. Air Force Office of Scientific Research (AOARD-09-4030).

References and Notes

(1) Campbell, I. M. *Energy and the Atmosphere*; Wiley: London, 1977.
(2) Wayne, R. P. *Chemistry of Atmospheres*; Oxford University Press: Oxford, U.K., 2000.
(3) Smith, J. A.; Cameron, E.; Ashfold, M. N. R.; Mankelevich, Y. A.; Suetin, N. V. *Diamond Relat. Mater.* **2001**, *10*, 358.
(4) Herzberg, G. *Proc. R. Soc., London, A* **1961**, *262*, 291.
(5) Fawzy, W. M.; Sears, T. J.; Davis, P. B. *J. Chem. Phys.* **1990**, *92*, 7021.
(6) Sears, T. J.; Frye, J. M.; Spiko, V.; Kraemer, W. P. *J. Chem. Phys.* **1989**, *90*, 2125.
(7) Hudgens, J. M.; DiGiuseppe, T. G.; Lin, M. C. *J. Chem. Phys.* **1983**, *79*, 571.
(8) DiGiuseppe, T. G.; Hudgens, J. M.; Lin, M. C. *J. Phys. Chem.* **1982**, *86*, 36.
(9) Parker, D. H.; Wang, Z. W.; Janssen, M. H. M.; Chandler, D. W. *J. Chem. Phys.* **1989**, *90*, 60.
(10) Black, J. F.; Powis, I. *J. Chem. Phys.* **1988**, *89*, 3986.
(11) Fu, H. B.; Hu, Y. J.; Bernstein, E. R. *J. Chem. Phys.* **2005**, *123*, 234307.
(12) Zhou, J.; Lin, J. J.; Shiu, W.; Pu, S.-C.; Liu, K. *J. Chem. Phys.* **2003**, *119*, 2538.
(13) Zhang, B.; Zhang, J.; Liu, K. *J. Chem. Phys.* **2005**, *122*, 104310.
(14) Zhang, B.; Yan, S.; Liu, K. *J. Phys. Chem. A* **2007**, *111*, 9263.
(15) Yamada, C.; Hirota, E. *J. Chem. Phys.* **1983**, *78*, 669.
(16) Amano, T.; Bernath, P. F.; Yamada, C.; Enao, Y.; Hirota, E. *J. Chem. Phys.* **1982**, *77*, 5284.
(17) Kawaguchi, K. *Can. J. Phys.* **2001**, *79*, 449.
(18) Davis, S.; Anderson, D. T.; Duxbury, G.; Nesbitt, D. J. *J. Chem. Phys.* **1997**, *107*, 5661.
(19) Bacon, J. A.; Pratt, S. T. *Chem. Phys. Lett.* **1999**, *311*, 346.
(20) Kelly, P. B.; Westre, S. G. *Chem. Phys. Lett.* **1988**, *151*, 253.
(21) Botschwina, P.; Flesch, J.; Meyer, W. *Chem. Phys.* **1983**, *74*, 321.
(22) Velasco, A. M.; Martin, I.; Lavin, C. *Chem. Phys. Lett.* **1997**, *264*, 579.
(23) Mebel, A. M.; Lin, S. H. *Chem. Phys.* **1997**, *215*, 329.
(24) Ishikawa, H.; Field, R. W.; Farantos, S. C.; Joyeux, M.; Koput, J.; Beck, C.; Schinke, R. *Annu. Rev. Phys. Chem.* **1999**, *50*, 443.
(25) Zwier, T. S. *J. Phys. Chem. A* **2006**, *110*, 4133.
(26) Dian, B. C.; Brown, G. G.; Douglass, K. O.; Pate, B. H. *Science* **2008**, *320*, 924.
(27) Boyarkin, O. V.; Lubich, L.; Settle, R. D. F.; Perry, D. S.; Rizzo, T. R. *J. Chem. Phys.* **1997**, *107*, 8409.
(28) Lester, M. I.; Pond, B. V.; Anderson, D. T.; Harding, L. B.; Wagner, A. F. *J. Chem. Phys.* **2000**, *113*, 9889.
(29) Robertson, W. H.; Johnson, M. A. *Annu. Rev. Phys. Chem.* **2003**, *54*, 173.
(30) Oka, T. *Adv. At. Mol. Phys.* **1973**, *9*, 127.
(31) Gottscho, R. A.; Field, R. W.; Bacis, R.; Silvers, S. J. *J. Chem. Phys.* **1980**, *73*, 599.
(32) Lin, J. J.; Zhou, J.; Shiu, W.; Liu, K. *Rev. Sci. Instrum.* **2003**, *74*, 2495.
(33) Dong, F.; Lee, S.-H.; Liu, K. *J. Chem. Phys.* **2000**, *113*, 3633.
(34) Riedel, J.; Yan, S.; Kawamata, H.; Liu, K. *Rev. Sci. Instrum.* **2008**, *79*, 033105.
(35) Tanarro, I.; Sanz, M. M.; Domingo, C.; Bermejo, D.; Santos, J.; Domenech, J. L. *J. Phys. Chem.* **1994**, *98*, 5862.
(36) Herzberg, G. *Molecular Spectra and Molecular Structure III*; van Nostrand Reinhold: New York, 1966.
(37) Chen, K.-M.; Yeung, E. S. *J. Chem. Phys.* **1978**, *69*, 43.
(38) Zhou, J.; Shiu, W.; Lin, J. J.; Liu, K. *J. Chem. Phys.* **2006**, *124*, 104309.
(39) Westre, S. G.; Kelly, P. B.; Zhang, Y. P.; Ziegler, L. D. *J. Chem. Phys.* **1991**, *94*, 270.
(40) Westre, S. G.; Gansberg, T. E.; Kelly, P. B.; Ziegler, L. D. *J. Phys. Chem.* **1992**, *96*, 3610.
(41) Westre, S. G.; Liu, X.; Getty, J. D.; Kelly, P. B. *J. Chem. Phys.* **1991**, *95*, 8793.
(42) King, G. W.; Hainer, R. M.; Cross, P. C. *J. Chem. Phys.* **1943**, *11*, 27.
(43) Schulenburg, A. M.; Alcaraz, Ch.; Grassi, G.; Merkt, F. *J. Chem. Phys.* **2006**, *125*, 104310.
(44) Crofton, M. W.; Jagod, M.-F.; Dehfuss, B. D.; Kreiner, W. A.; Oka, T. *J. Chem. Phys.* **1988**, *88*, 666.
(45) Heinze, J.; Heberle, N.; Kohse-Hoinghaus, K. *Chem. Phys. Lett.* **1994**, *223*, 305.
(46) Liu, K. *Phys. Chem. Chem. Phys.* **2007**, *9*, 17.

JP902969V